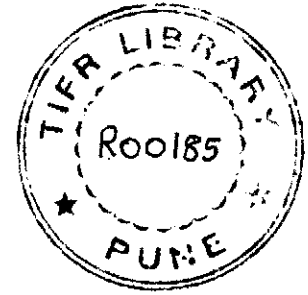


# GMRT antenna power pattern in L band

Data from 27-28 December 2000

*Nimisha G. Kantharia & A. Pramesh Rao*

July 20, 2001



## 1 Aims

1. To study the shape of the GMRT antenna primary beam - both the elevation and azimuth beams and obtain the half power beam width.
2. To obtain the best polynomial fit to the GMRT antenna primary beam shape required for primary beam response correction in the final analysis using the task PBCOR in AIPS.
3. To study the variation in the pointing offsets with elevation.
4. To study the effect of the FPS position on the elevation beam shape.

## 2 Introduction

The L band feed consists of a corrugated horn designed and made by the Raman Research Institute. This type of feed has a high aperture efficiency and low cross-polarization levels. The feed receives two linear polarizations which are then further processed. The L band is the only band at GMRT where the two orthogonal linear polarizations are processed and available to the astronomer. As with the rest of the GMRT bands, this feed is also a prime focus feed, positioned at the focus of the parabolic dish and mounted on a turret. The front-end electronics are also mounted on the turret. The flare angle of the corrugated horn is  $120^\circ$ . The feed illuminates the 45-m mesh reflector which has a radially varying mesh size. The inner 1/3rd has a mesh size of 10mm, the middle 1/3rd of 15mm and the outer 1/3rd of 20mm. The wide-band feed has a VSWR  $< 2$  for a bandwidth of 580 MHz - ranging from 1000 MHz to 1580 MHz. This band is divided into 4 sub-bands, each of bandwidth 140 MHz centred on 1060, 1170, 1280 and 1390 MHz. A bypass mode which allows the usage of the entire 580 MHz bandwidth also exists. For our experiment, we used the 1060 MHz and 1280 MHz sub-bands.

The entire experiment was divided into four parts to study four aspects related to the L band beam. The 130 MHz polarization channel was used. The first part concerned the study of the beamshape in both the altitude and azimuth directions and to obtain the half power beamwidth. For this we obtained a one-dimensional cut in elevation and azimuth by observing a grid of points about a strong point source. While the azimuth beam is fairly symmetric, the elevation beam was found to be skewed. The second part was to use this data and find the best polynomial fit to the beamshape. This is required for correcting the GMRT data for the primary beam gain variation. An eight-order polynomial fit was found to fit the azimuth beam well and the results are presented here. In the third part to study the variation in elevation pointing offsets with source elevation, we tracked a strong point

source through a run and noted down the offsets. The offsets do not vary significantly, but they do show a systematic variation of  $\leq 4'$ . Lastly, to obtain an optimum position for the FPS, we wanted to do the fourth part of the experiment by rotating the feed turret to obtain a more-symmetric elevation beam. The data and discussion can be found in another report.

### 3 - On the Observational Data

For the first and second part of the experiment, we observed a one-dimensional grid of points in elevation and azimuth centred on a strong point source (e.g 3C48) as shown in Fig 1. All the antennas except a couple were made to observe the grid points. The remaining two antennas were used as reference and moved to another sub-array and made to track the point source. The data was recorded. In the data analysis, the normalized cross-correlations between the reference antennas and the rest of the antennas were used to obtain the beam shape. Details of the experimental setup was as follows:

Table 1: Experimental details

Reference antennas	C01, C05
Sub-band	1280 MHz
LOI	1210 MHz
IF BW	32 MHz
LO4	70 MHz
BBW	8 MHz
LTA	4 sec
ALC	ON
Total grid points	11
Grid spacing	6'
Total grid extent	$\pm 30'$
Data length per point	2 min

For implementing the above procedure, we made a command file with the appropriate ONLINE commands for observing each grid point for 2 minutes. After setting up the DAS and starting the project, we ran the command file, part of which is shown here:

```
gts'ELE1'
sndsacsrc(1,1h)
trkelof(-30')
trksac(1,1h)
strtndasc
time 2m
stpndasc
```

The above few lines would observe the southern-most elevation grid point and acquire data for 2 minutes before moving on to the next command and hence represents one module of the command file. 'ELE1' is one of the dummy names created to recognise the grid

point and hence ease the offline data analysis. The coordinates of ELE1, ELE2... were the same as the point source that we were observing, in this case, 3C48 ( $S_{20cm} = 16.5$  Jy). It was important to remind the antennas to move to the point source before moving from one grid point to another. By running a command file made of many such modules, we acquired data for the one-dimensional grid of points. When the entire grid was covered, then the project was stopped and the data examined. A similar exercise was done for a grid in the azimuth.

For the third part of the experiment, we observed a coarser one-dimensional grid of points in elevation. The RF, IF, BB settings are given in following table: (The fractional

Table 2: Experimental details

Reference antennas	C01, C05
Sub-band	1060 MHz
LOI	1030 MHz
IF BW	32 MHz
LO4	66.4 MHz
BBW	8 MHz
LTA	4 sec
ALC	ON
Total grid points	7
Grid spacing	5'
Total grid extent	$\pm 25'$
Data length per point	2 min

numbers for LO4 is because we started this expt at the end of an observing session which used the above settings) The grid of seven points was repeatedly cycled through while tracking a strong point source, in this case, 3C286 ( $S_{20cm} = 15$  Jy) through one observing run in order to catch the source at different elevations and study the variation in pointing offset. The cross-correlations with the reference antenna were used in the offline analysis. We also cycled through an azimuth grid of points, infrequently compared to the elevation grid to check for any azimuth offset dependence on elevation.

In the fourth part of the experiment, we scanned across a strong point source in the correlation mode and the relative sidelobe levels were examined. If the sidelobes were found to be asymmetric then the feed was rotated and the scan across the source taken again. The most optimum position of the feed was determined from the most symmetric sidelobe pattern obtained. More details of this part, the data and its analysis will be given in another report.

Using the subarray facility in ONLINE, we assigned the reference antennas, C01 and C05 to one subarray and the rest of the antennas (all available antennas were used in the experiment, however we concentrated mainly on the central square antennas) into another subarray, thus enabling independent control. C01 and C05 were used to track the source (3C48/3C286) and the rest of the antennas observed the grid points and the data were recorded.

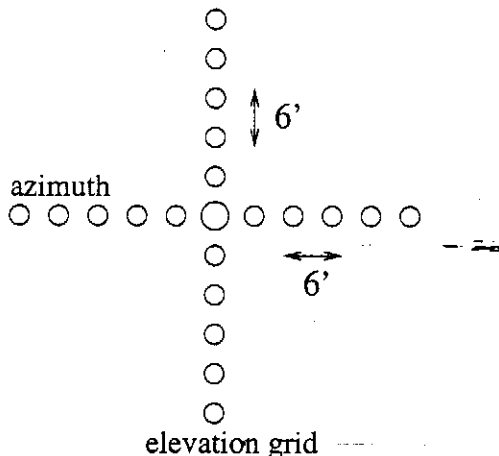


Figure 1: Grid of points observed along elevation and azimuth axes

### 3.1 Offline Analysis

The data obtained, thus, was analysed using locally developed software. *xtract* (author: Sanjay Bhatnagar) was used to time-average each of the 2m scans. No editing was effected before averaging. No channel-averaging was done. This data was written out in a *qdp* data file format. Since the normalized correlation coefficients would be in voltage units for the antenna under consideration (the reference antenna give a constant signal which is correlated with the signal from the grid-observing antenna), these were squared using a routine written by one of us (NGK) to obtain the power pattern. The observed primary beam pattern for first three parts were fitted with a functional form. We fitted a polynomial to these patterns in the software package *qdp* using a procedure written by one of us (APR). The procedure uses the polynomial-fitting routine within *qdp* after removing any pointing offset that the particular antenna may have. It invokes the *qdp* fitting routine and prompts the user to specify the pointing offset and the coefficients for the even indices of a polynomial to fit the beamshape i.e. coefficients for a constant, a quadratic, a biquadratic and a bicubic terms. The polynomial that fitted the azimuth beam well was:

$$P = 1 + a x^2 + b x^4 + c x^6 + d x^8 \quad (1)$$

where  $x = x' - x_0$  where  $x'$  is the (distance from the peak in arcmin \* freq in GHz) and  $x_0$  is the pointing offset and  $a, b, c, d$  are the coefficients that we are interested in. The best model outputs are listed below. We also checked the goodness of gaussian fits to the beamshapes to examine the relative goodness of the eighth order polynomial and gaussian fits. A similar test was conducted using a sixth-order and 10th order polynomials. The eighth-order polynomial was found to give the best fit amongst these. The functional form for the gaussian that was fitted was:

$$G = \frac{1}{\sigma \sqrt{2\pi}} a \exp\left(-\frac{1}{2}\left(\frac{x-b}{\sigma}\right)^2\right) \quad (2)$$

where  $a$  is the peak power,  $b$  is the pointing offset and  $\sigma$  is the dispersion.  $HPBW = 2.354 * \sigma$ .

For the third part of the experiment, the shift in the peak of the beam as the source elevation changes was examined by fitting a gaussian to each set of grid points about the source. This was effected in *qdp*. This procedure was done for a few antennas (C09, C14, C13, C04, C02, E05) and the offsets noted.

## 4 Results

The primary beam for both the elevation and azimuth grids are shown in Figures 2 to 5. Polynomial fits are superposed on the observed beam shape in Figs 2 and 3 whereas a gaussian fit is superposed on the observed beam in Figs 4 and 5.

### 4.1 The azimuth and elevation beams: symmetry

Examining Figs 4 and 5 which show the primary beams for the antennas C04, C09, C13, C14, it is fairly obvious that the azimuth beams are fairly symmetric compared to the elevation beams. For example, consider the elevation and azimuth beams for C09 in Figs 2 and 3. The azimuth beam is well-fitted by a gaussian and is symmetric while the elevation beam shows visible asymmetry. This is obvious in the case of the other antennas in Figs 4 and 5 also. Since the azimuth beam is symmetric down to  $< 10\%$  points of the beam whereas the elevation beam displays asymmetry upto 30% points of the beam, the asymmetry in the latter could be due to the FPS position not being the optimum. Since the feeds are mounted on a turret which is rotated for observing different frequencies, if the FPS position is not correct, the elevation beam can display such asymmetries. The fourth part of the experiment was devised to obtain a more symmetric elevation beam.

### 4.2 The half power beam width (HPBW)

Gaussian fits to the power pattern (Figs 4, 5) yielded the following HPBW for the 1280 MHz sub-band.

Azimuth beamwidth was found to lie in the range 25.4' to 26.7'.

Elevation beamwidth was found to lie in the range 26.1' to 28.3'. Please note that all our experiments were done using only the 130 MHz polarization channel.

Since the elevation beams show some skewness, we consider only the HPBW obtained from the azimuth beams. The mean value is  $26.1' \pm 0.7'$ . It should be scaled by the frequency from 1280 MHz to obtain the HPBW for the other frequencies and matches the values obtained using the total power scans (Vasant Kulkarni) across strong point sources (e.g. Virgo A, Cygnus A, Cas A).

If the GMRT antenna is a uniformly-illuminated circular aperture with diameter  $D$ , then its HPBW at a wavelength  $\lambda$  is given by  $1.22 \frac{\lambda}{D}$  for uniform illumination. This gives a value of  $\sim 22'$  for the beam at 1280 MHz. However, the L-band feeds are tapered to obtain a compromise between the tapering efficiency and the spillover efficiency. To reduce the

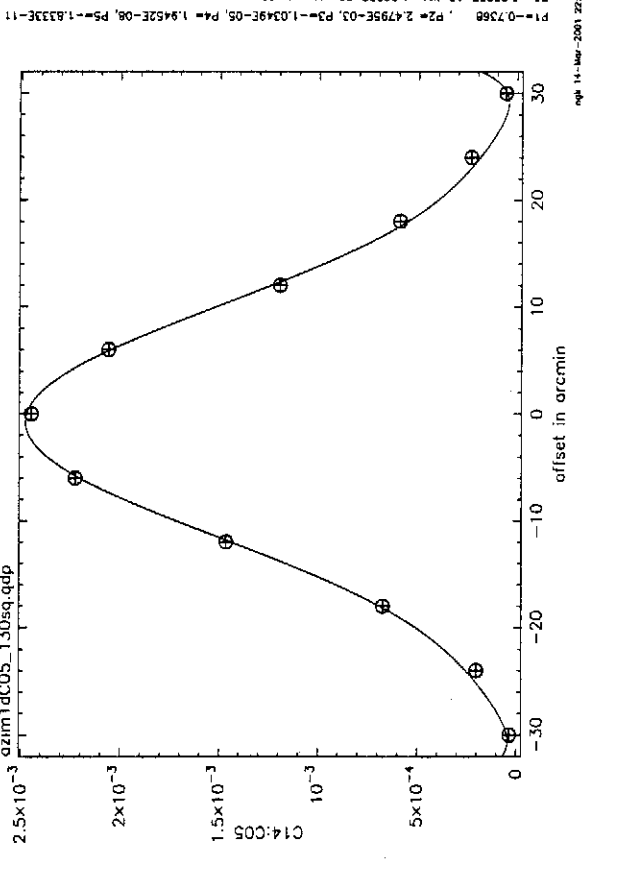
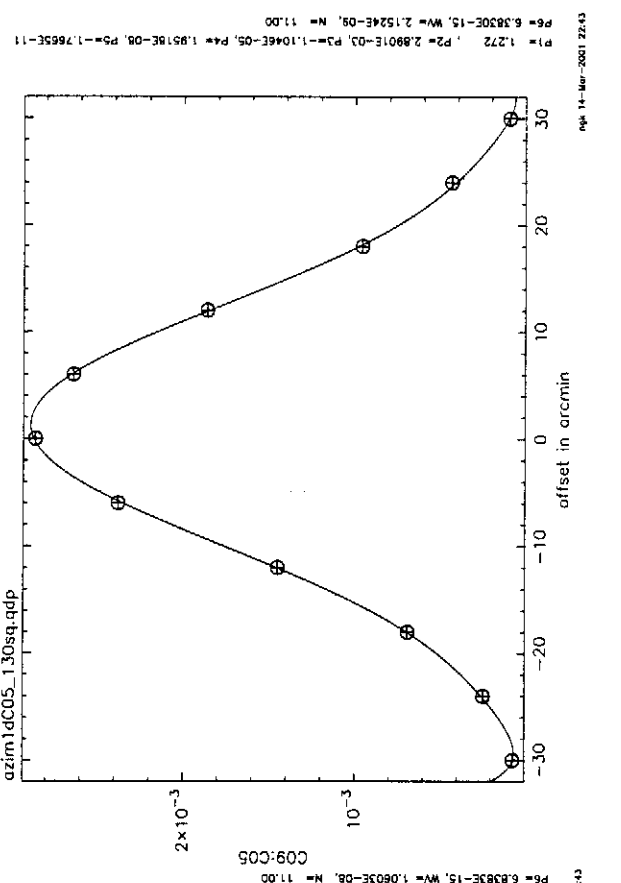
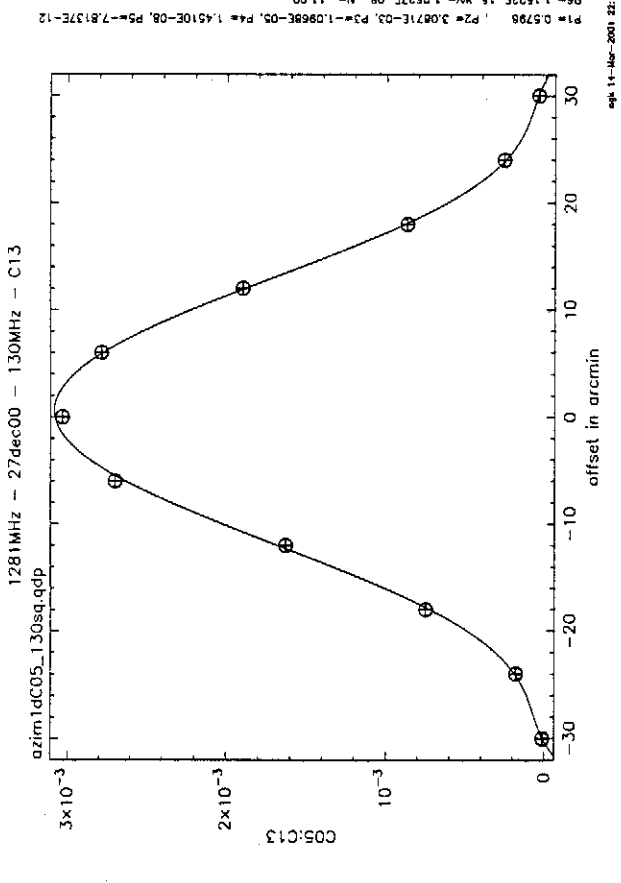
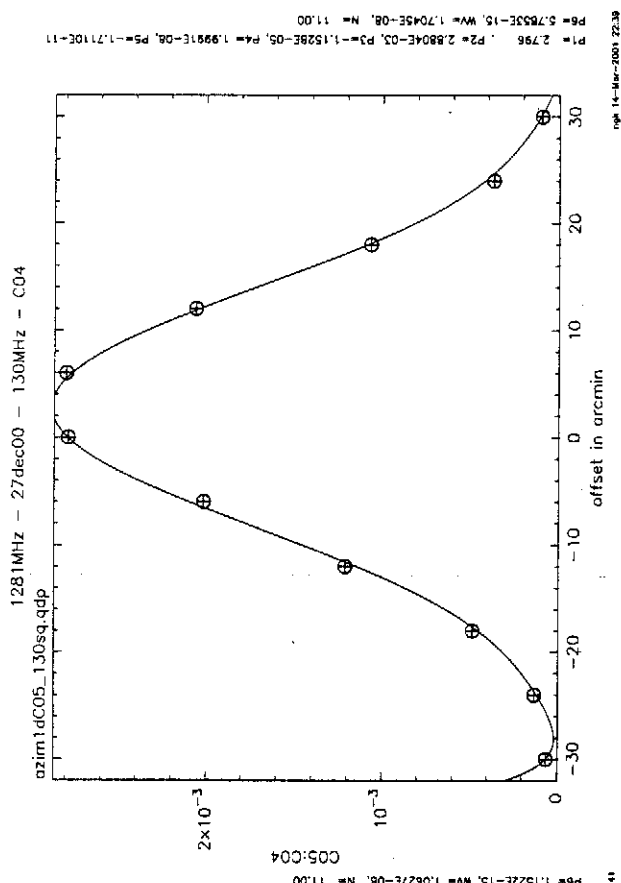


Figure 2: Eighth-order Polynomial fit to azimuth grid. The points are the observed data whereas the solid line shows the eighth order polynomial fit.

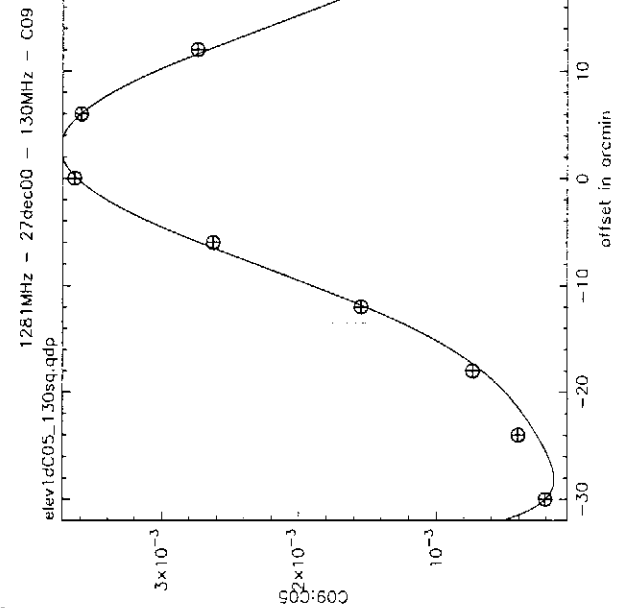
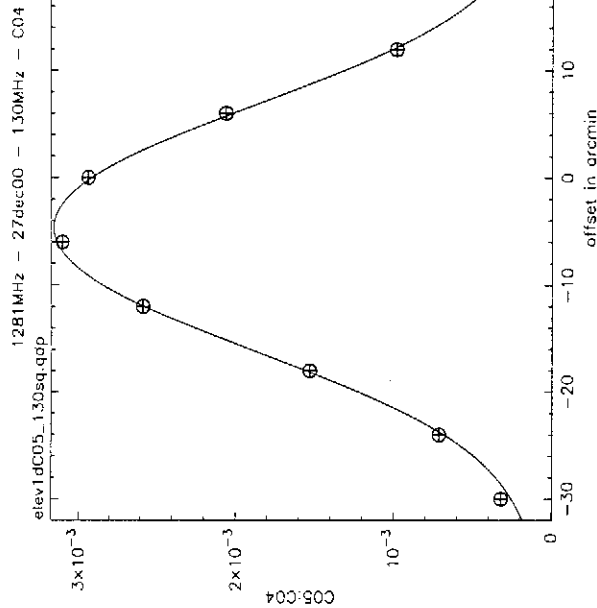
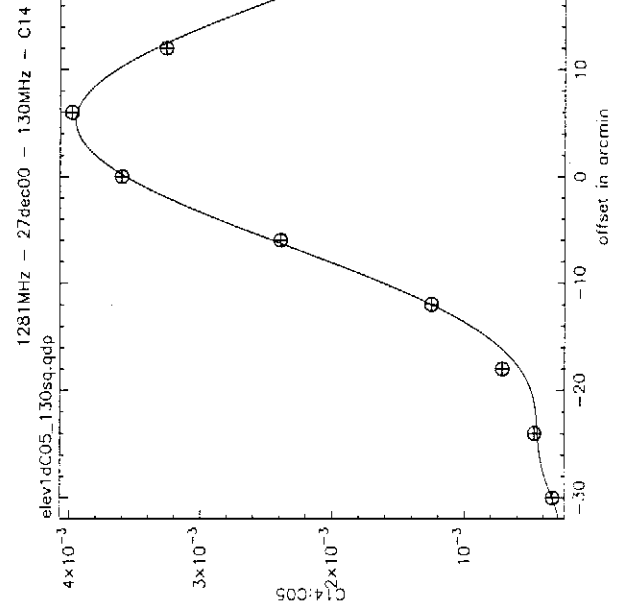
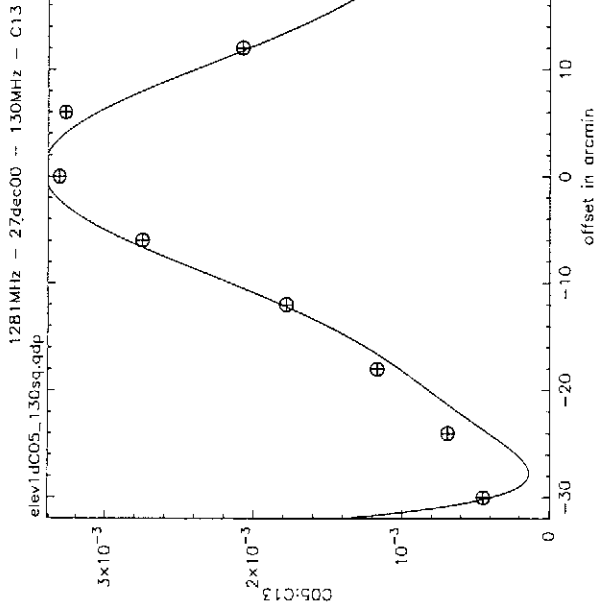


Figure 3: Polynomial fit to elevation grid. The points show the observed data whereas the solid line shows the eighth order polynomial fit.

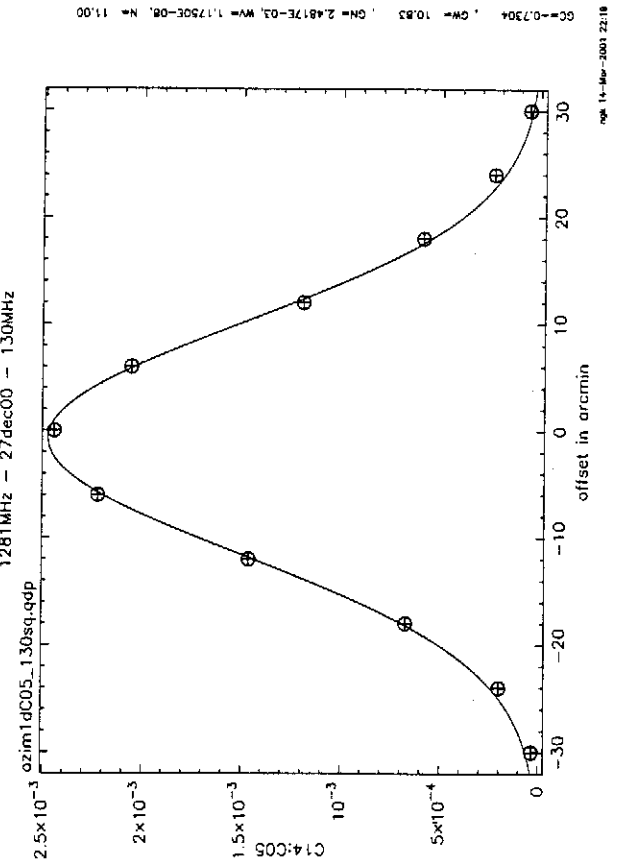
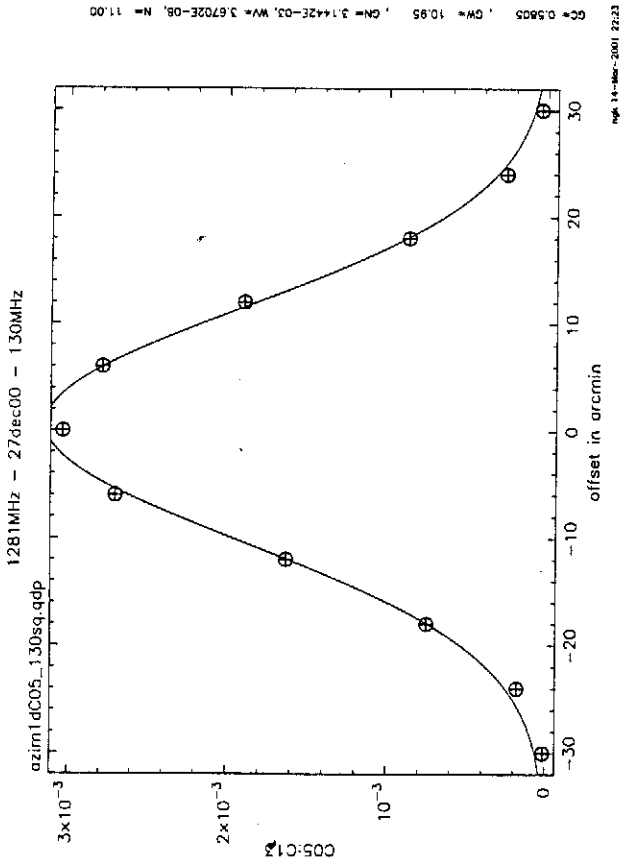
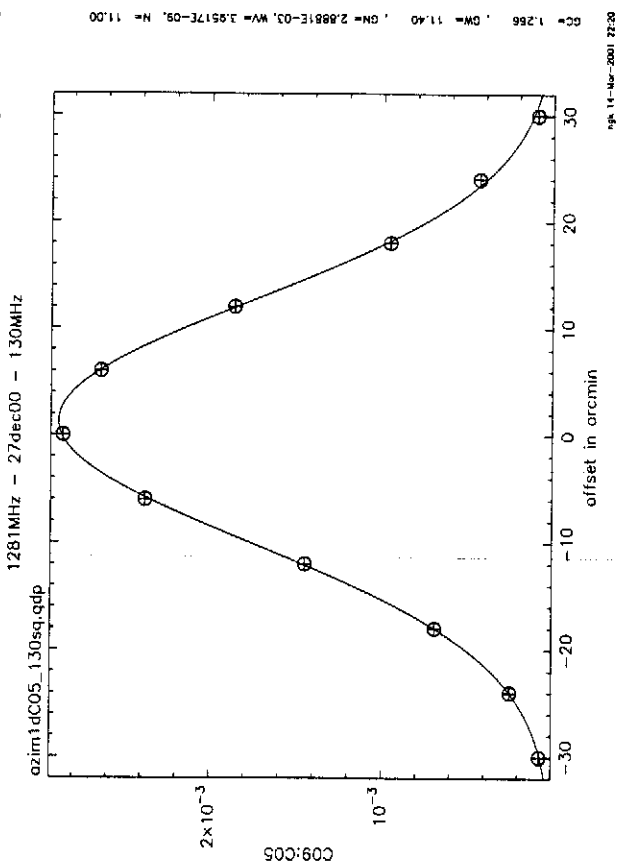
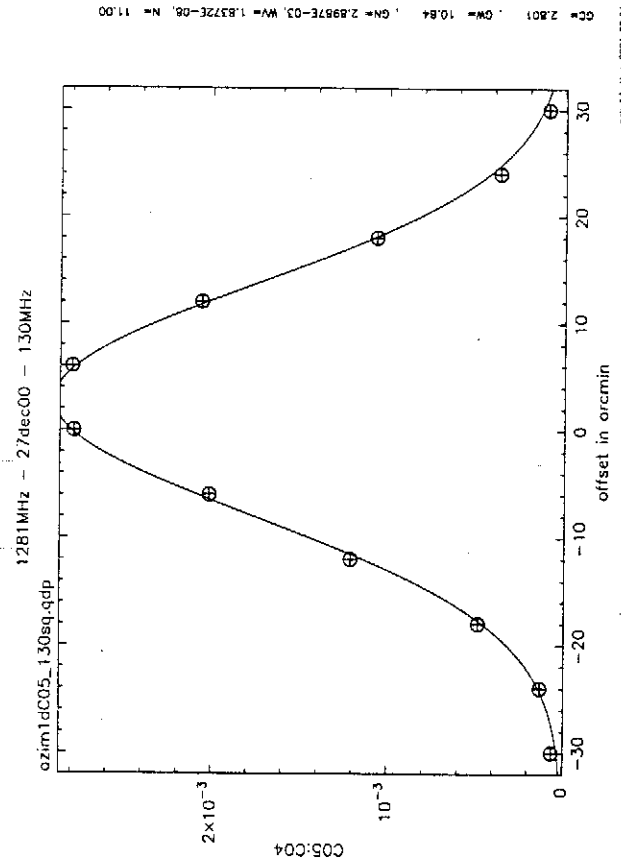
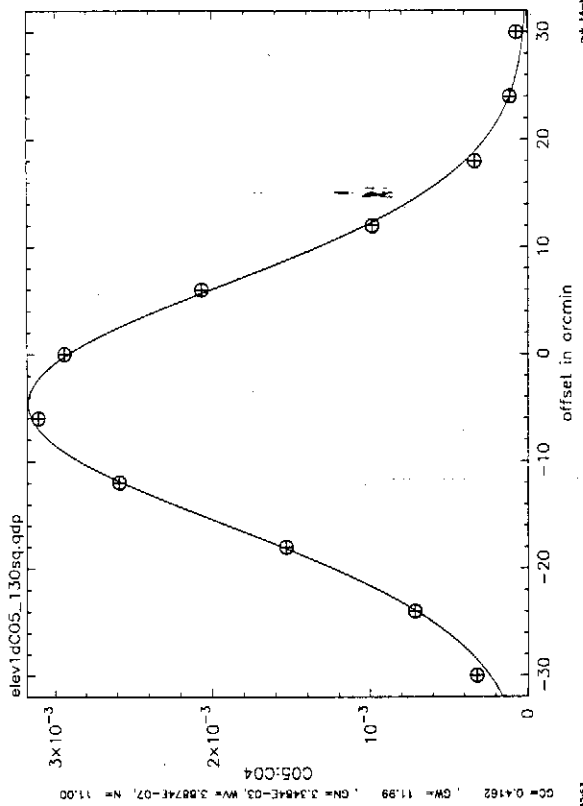


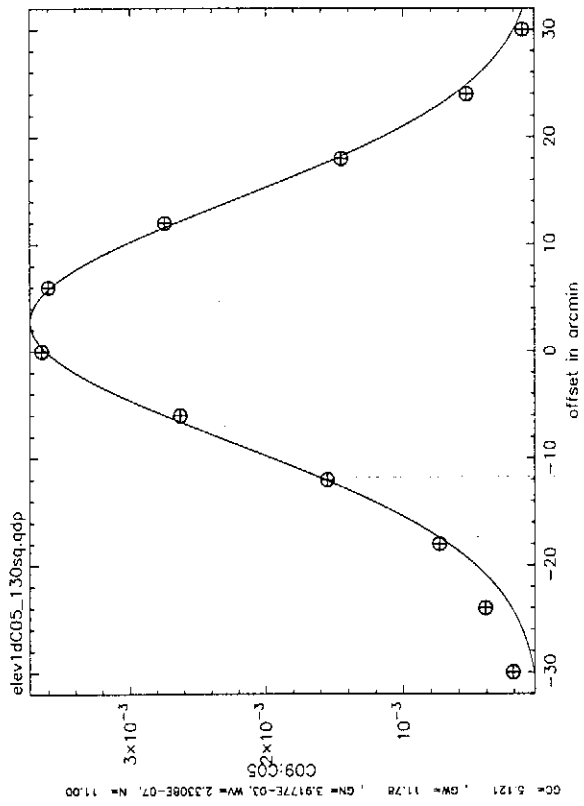
Figure 4: Gaussian fit to azimuth grid



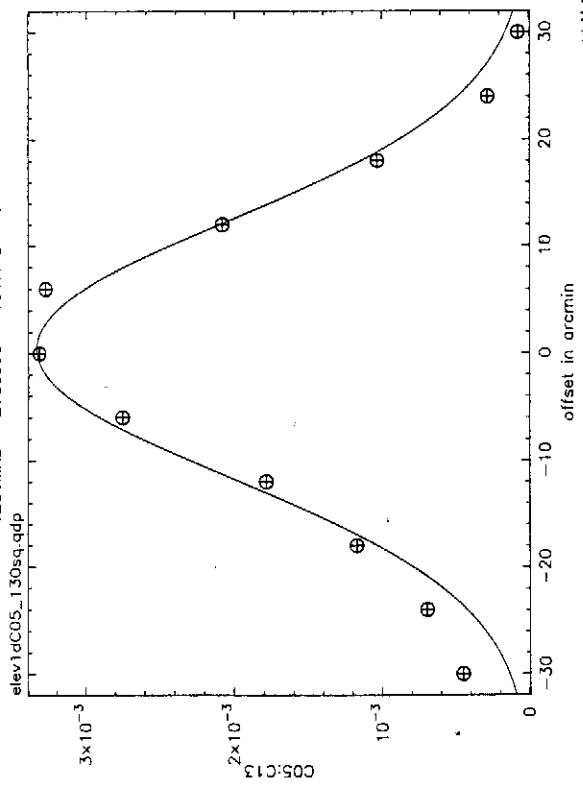
1281MHz - 27dec00 - 130MHz - C04



1281MHz - 27dec00 - 130MHz - C09



1281MHz - 27dec00 - 130MHz - C13



1281MHz - 27dec00 - 130MHz - C14

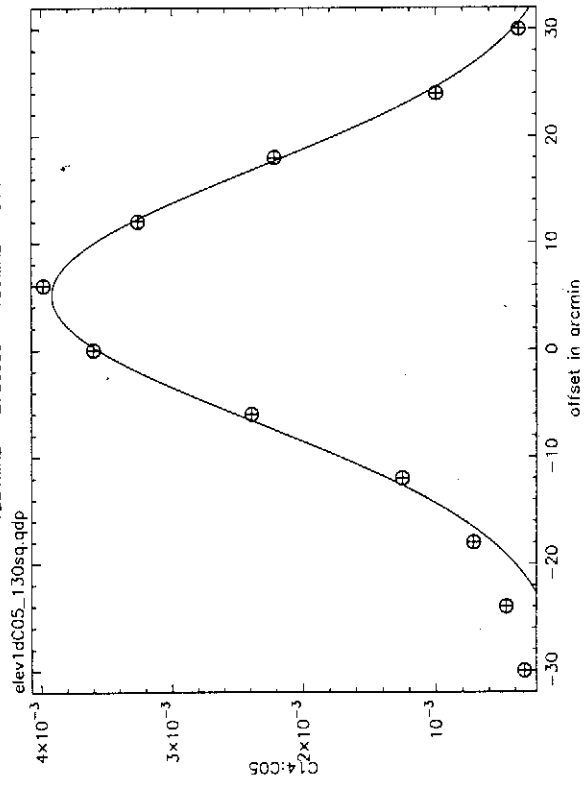


Figure 5: Gaussian fit to elevation grid

spillover, the aperture illumination is tapered, resulting in a wider beam, in this case a HPBW  $\sim 26'$  at 1280 MHz.

**Work to be done:** It would be useful to repeat the one-dimensional grids along azimuth and elevation axes for the various sub-bands within L band and confirm the frequency scaling to the beamwidth and the present result.

### 4.3 Functional fits to the observed Beams required for primary beam gain correction

Below are tabulated the variance for the gaussian and polynomial fits to the azimuth beams for a few central square antennas. The variance for both an eighth-order and sixth-order polynomials are listed to show that the eighth-order gives the best fit to the beamshape.

Table 3: Comparing the variance of a gaussian, an eighth order polynomial and a sixth order polynomial fit to the primary beam.

Antenna	Variance		
	Gaussian	8th order polynomial	6th order Polynomial
C04	184	170	301
C09	40	22	140
C13	367	106	108
C14	118	106	192

The observed beams were approximated by eighth-order polynomials and the coefficients obtained. The eighth-polynomial functional form was fitted to the observed azimuth beams for a few antennas: C04, C09, C13, C14, S03 and W06 and the mean values for the coefficients obtained which are tabulated in table 4.3. A similar exercise was done for the elevation beams also and the mean coefficients listed in the Table 4.3 obtained from C04, C09, C14 and W06.

Table 4: Eighth order polynomial fit coefficients for the L band primary beam

Coefficient	Azimuth beam		Elevation beam
	Value	Uncertainty ( $\sim 1\sigma$ )	Value
a	$-2.27961 \times 10^{-3}$	$0.01 \times 10^{-3}$	$-2.28152 \times 10^{-3}$
b	$2.14611 \times 10^{-6}$	$0.24 \times 10^{-7}$	$2.21387 \times 10^{-6}$
c	$-9.7929 \times 10^{-10}$	$2.6 \times 10^{-10}$	$-10.0982 \times 10^{-10}$
d	$1.80153 \times 10^{-13}$	$0.76 \times 10^{-13}$	$1.78146 \times 10^{-13}$

The uncertainties are from the measured values. The peak-to-peak variation in the coefficients for the different antennas was noted and rms uncertainty obtained for the azimuth beam. Since we are not using the elevation beam; we have not calculated the error bars. Since these coefficients are normalized by the observed frequency, they need to be scaled to the appropriate frequency in the L band to get the desired polynomial fit to

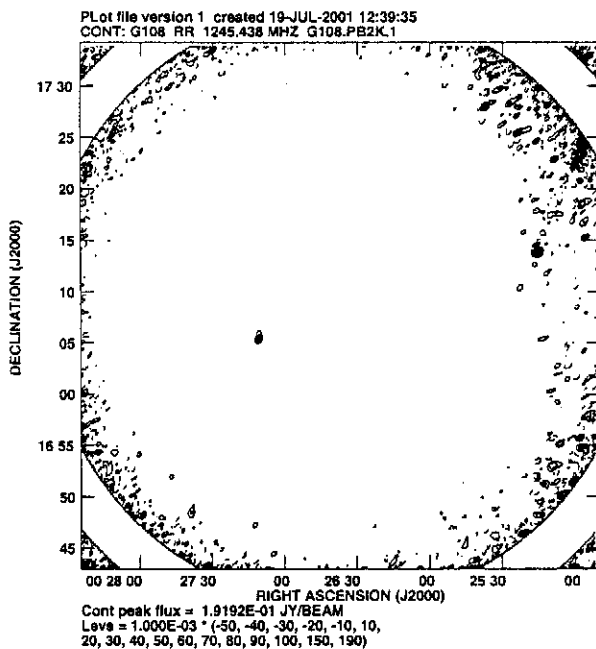


Figure 6: Primary beam gain correction on a field observed with GMRT at 1280 MHz.

the primary beam response. The  $x$  in Eq 3 is in terms of the frequency and the distance from the beam center in arcmin. The scaling is taken care of by the task PBCOR in AIPS which is discussed briefly in the next subsection. The correction should be effected to only 10% points of the main beam. Going to lower points is not advisable since the signal-to-noise ratio in those regions also degrades considerably and hence the image is not usable.

#### 4.4 PBCOR in AIPS

The above coefficients are to be provided to the task PBCOR in AIPS (Astronomical Image Processing System) for implementing the primary beam correction to the data in the image plane. We entered the coefficients in the DPARM adverbs in PBCOR and applied it to an image at 1280 MHz. The result is shown in Fig 6.

The field shown in Fig 6 is clean with only a couple of sources visible: one to the east of the phase center and another north-west of the phase centre which is almost buried in the beam edge noise. The edges of the beam are noisy due to the poor signal-to-noise ratio. The noise which is seen in the four corners of the image is due to the polynomial fit rising at the beam-edges much below the 5% points. Since this is not the region of the beam that we are interested in, it can be ignored except for the aesthetically-compromised image! We measured the peak brightness of three point sources visible in our image and compared the flux to that found from the NVSS image downloaded from the net. This was done to check the functioning of the polynomial fit. The uncorrected and corrected flux densities of the sources are also tabulated.

From Table 4.4, the increase in the flux densities effected by the primary beam cor-

Table 5: Primary beam gain correction

$\alpha_{2000}$ hh mm ss	$\delta_{2000}$ ° ' "	S1(1280 MHz)		S2(1420 MHz)	S1 (After PBCOR) /S2
		Before PBCOR	After PBCOR	NVSS	
00 25 16	17 13 51	42 mJy	214 mJy	268 mJy	0.80
00 27 11	17 05 30	54 mJy	70 mJy	92 mJy	0.76
00 25 37	17 28 01	6 mJy	68 mJy	188 mJy	0.36

rection is evident in columns 3 and 4. The NVSS values are listed in column 5 whereas column 6 gives the ratio of the gain-corrected flux densities from our 1280 MHz map and the NVSS 1420 MHz map. The first and second sources are clearly visible in Fig 6 whereas the third source is buried in the noise and not clearly discernible here. So considering only the first two sources, the flux density seems to have been properly gain corrected since the ratio is constant at  $\sim 0.8$ . The lower 1280 MHz flux densities are most probably due to an amplitude scale error. The last point is  $\sim 1\sigma$  in the uncorrected map and hence should not be overemphasized. Hence to first level, the primary beam correction seems to be working.

**Work to be done:** Scaling the primary beam coefficients to other frequencies has to be checked out. It would be useful to use the above coefficients in AIPS and correct the other sub-band frequencies and compare with published maps like the NVSS.

#### 4.5 Variation in Pointing offsets as a function of Source Elevation

The offsets obtained by fitting a gaussian to each grid was plotted against the elevation of the source as shown in Fig 7 & 8. We find that the elevation pointing offsets vary within  $4'$  for five of the six antennas that we studied. The figures (Fig 7) show these results clearly. The errors on the data when C01 was used as the reference antenna are somewhat lower than those for C05 as reference antenna and a slow variation in the elevation pointing offset as the elevation of the source changes is evident in the data. Unfortunately we did not have data between hour angles  $-1h$  and  $2h$  ie near the transit of the source - however the trend is clearly seen. The jump in some of the offsets after transit ie after crossing elevation of  $90^\circ$  is due to an understood servo problem which is being presently addressed by the engineers. The azimuth data (Fig 8) has been given for comparison and as expected there is little change in the offsets with elevation.

**Work to be done:** 1) This experiment needs to be repeated a couple of times to try and get a functional form for the variation in pointing as a function of elevation. 2) Software for the data analysis needs to be developed.

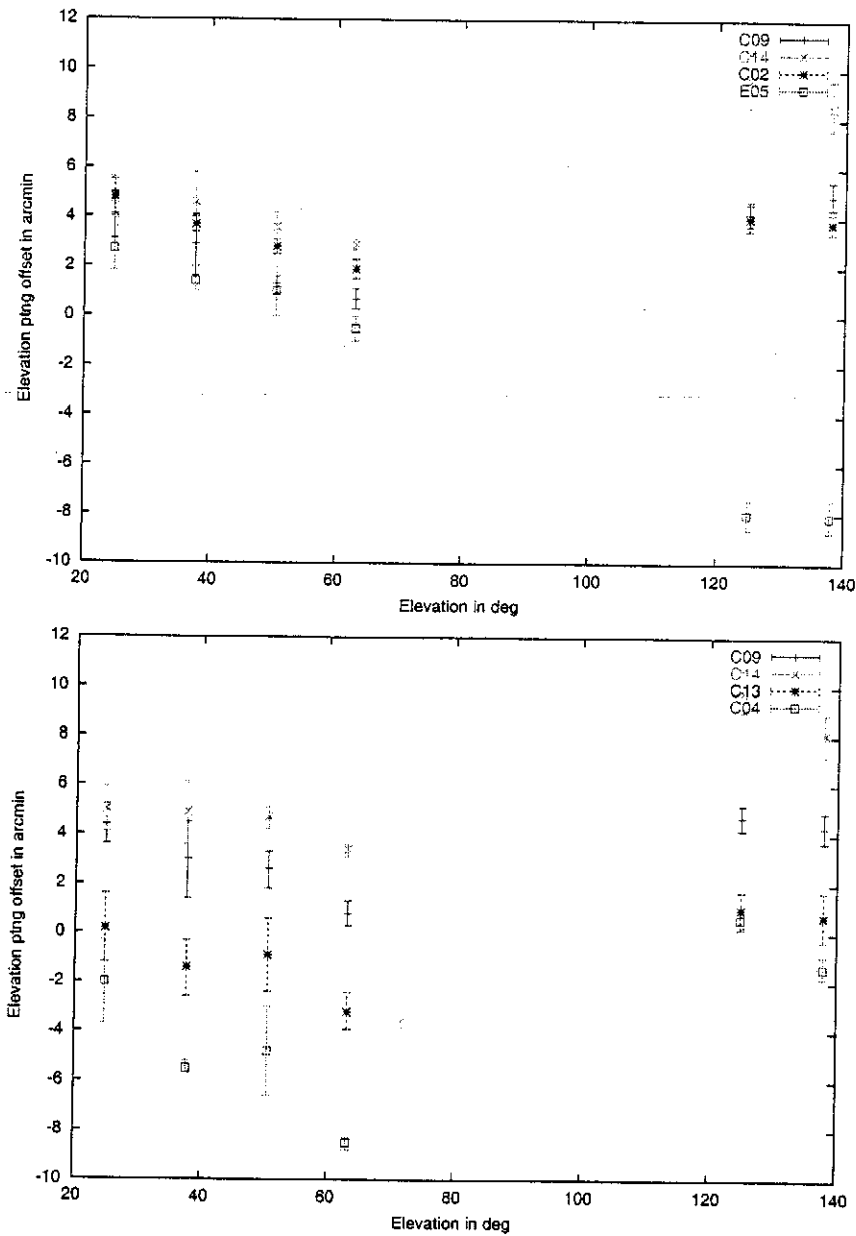


Figure 7: Variation in pointing offsets as a function of elevation. The elevation has been taken to run from 0 to 180° for convenience. For any  $x > 90^\circ$  in the figure,  $elevation = (x - 90)^\circ$ . The top panel shows the elevation offsets for four antennas C09,C14,C02,E05 where C01 has been used as the reference antenna. The bottom panel shows the same for C09,C14,C13,C04 using C05 has the reference antenna. A slow variation in pointing with elevation is observed.

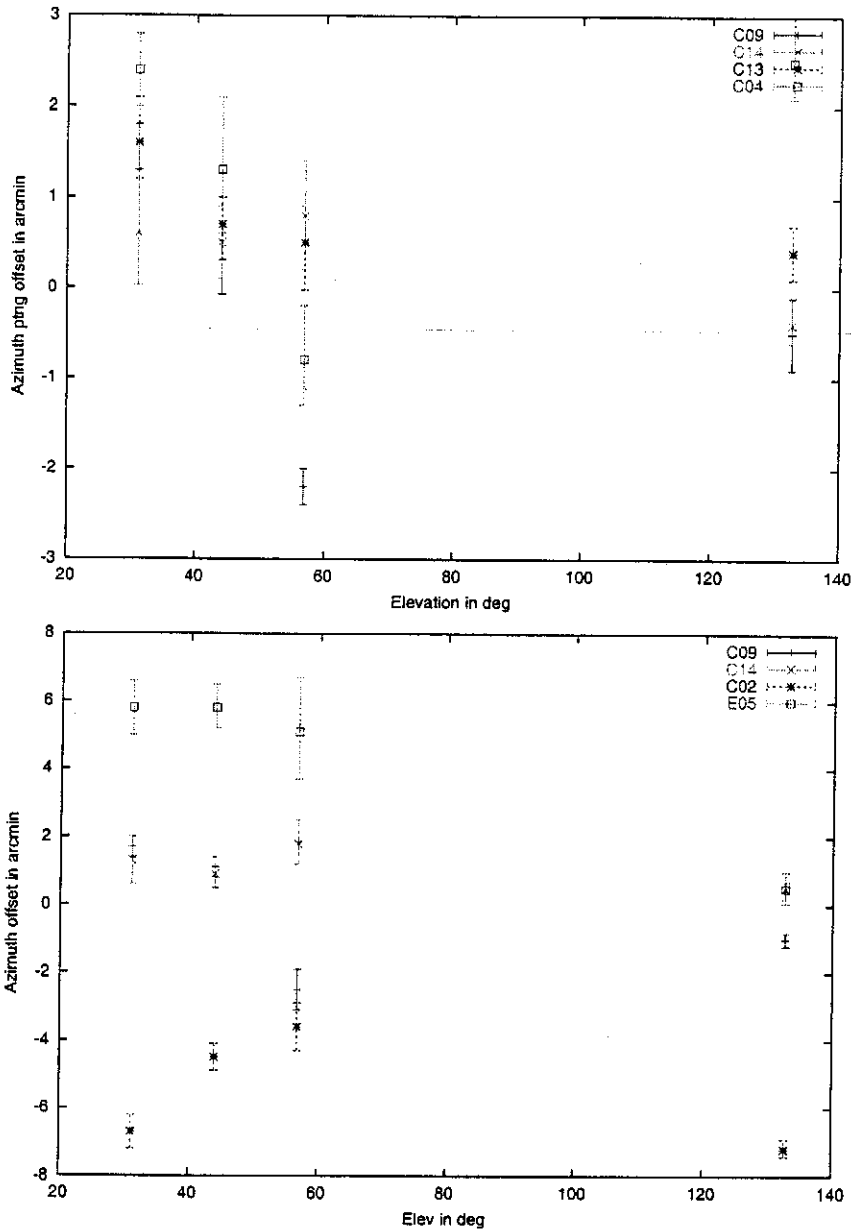


Figure 8: Figure shows the azimuth pointing offsets as a function of elevation of the source for C09,C14,C13,C04 using C05 as the reference antenna. Note that the variation for most antennas is  $< 2'$ . The lower panel is for C01 as reference and includes two other antennas

## 5 Summary

The entire experiment was divided into four parts to study four aspects related to the L band beam. The 130 MHz polarization channel was used. The first part concerned the study of the beamshape in both the altitude and azimuth directions and the half power beamwidth at 1280 MHz was obtained. For this we obtained a one-dimensional cut in elevation and azimuth by observing a grid of points about a strong point source. While the azimuth beam is fairly symmetric, the elevation beam was found to be skewed. The half power beamwidth at 1280 MHz was found to be  $26.1' \pm 0.7'$ . The second part was to use this data and find the best polynomial fit to the beamshape. This is required for correcting the GMRT data for the primary beam gain variation. An eight-order polynomial fit was found to fit the azimuth beam well and the mean coefficient values are presented here. In the third part to study the variation in elevation pointing offsets with source elevation, we tracked a strong point source through a run and noted down the offsets. The offsets do not vary significantly, but they do show a systematic variation of  $\leq 4'$ . Lastly, to obtain an optimum position for the FPS, the fourth part of the experiment by rotating the feed turret to obtain a more-symmetric elevation beam was devised. The data and discussion can be found in another report.

NGK thanks Sanjay Bhatnagar and G. Shankar for useful discussions. Presently, more data and information has been gathered following some more system tests regarding the L band beamshape and the optimum position of the feed positioning system. These results will be presented in a separate report.

## 6 References

Shankar G., SERC School lecture series..., chapter 3.

# GMRT Antenna Primary Beams Gain Correction Factors (240, 325, 610 MHz)

*Nimisha G. Kantharia & A. Pramesh Rao*

**Addendum to Technical Report R00185**

June 30, 2003

## 1 Introduction

In the technical report entitled ‘GMRT antenna power pattern in L band’, we had noted down the procedure adopted for finding out the coefficients of a polynomial function characterizing the primary beam for L band and the results. At that time, we had developed some basic software but the entire procedure of analysing the data was fairly labourious limiting us to a few antennas at the best. In this addendum, we describe the modified software which allows us to find polynomial fits to all ‘good’ antennas with minimum user intervention. We have extended this exercise to 240 MHz, 325 MHz and 610 MHz bands also and we present the results here. We have also repeated the exercise for the L band. This procedure can be used to characterize the primary beam when the data is taken along 1-dimensional grids in elevation and azimuth. In the longer run, it will be useful to obtain fits to 2-dimensional scans and characterise the primary beam especially at the lower frequencies.

## 2 Procedure

We obtained data at 240 MHz on 16,17 August 2001 and October 31, November 1 2002; at 325 MHz on July 15, 2001; at 610 MHz on 17 August 2001, 22, 24 September 2001 and 1 November 2002; at 1280 MHz on 28 June 2002. Data were obtained along both elevation and azimuth grids. A sample command file run by the control system, ONLINE for obtaining 610 MHz data is shown in Fig 1. The command files shows that the source 3C147 was tracked by two reference antennas which were kept in one subarray. The rest of the antennas were pointed at the different grid positions denoted in the file by ELE1, ELE2 and so on. A total grid extent of  $-150'$  to  $+150'$  in elevation and  $-180'$  to  $180'$  in azimuth in steps of  $15'$  was used at 240 MHz; an extent of  $-120'$  to  $120'$  in elevation and an extent of  $-180'$  to  $+180'$  azimuth in steps of  $12'$  was used at 330 MHz and an extent of  $-60'$  to  $+60'$  in elevation and  $-72'$  to  $+72'$  in azimuth in steps of  $12'$  was used at 610 MHz. A larger extent was used for the azimuth grid since the grid spacing was kept constant. The  $\cos(\text{elevation})$  effect was the reason for increasing the grid extent. Default frequency settings were used for all the bands.



```

cmode 1
suba 4
lnkndas

addlist '/temp2/data/source/bea
mshape.list'

gts '3c147'
goout
gosacout
sndsacsrc(1,12h)
trkazof(0')
trksac(1,1h)

gts'ELE1'
sndsacsrc(1,1h)
trkelof(-60')
trksac(1,1h)
strtndasc
time 2m
stpndasc

gts'ELE2'
sndsacsrc(1,1h);
trkelof(-48');
trksac(1,1h)
strtndasc
time 2m
stpndasc

gts'ELE3'
sndsacsrc(1,1h);
trkelof(-36');
trksac(1,1h)
strtndasc
time 2m

gts'ELE4'
sndsacsrc(1,1h);
trkelof(-24');
trksac(1,1h)
strtndasc
time 2m
stpndasc

gts'ELE5'
sndsacsrc(1,1h);
trkelof(-12');
trksac(1,1h)
strtndasc
time 2m
stpndasc

```

```

gts'ELE6'
sndsacsrc(1,1h);
trkelof(0');
trksac(1,1h)
strtndasc
time 2m
stpndasc

gts'ELE7'
sndsacsrc(1,1h);
trkelof(12');
trksac(1,1h)
strtndasc
time 2m
stpndasc

gts'ELE8'
sndsacsrc(1,1h);
trkelof(24');
trksac(1,1h)
strtndasc
time 2m
stpndasc

gts'ELE9'
sndsacsrc(1,1h);
trkelof(36');
trksac(1,1h)
strtndasc
time 2m
stpndasc

gts'ELE10'
sndsacsrc(1,1h);
trkelof(48');
trksac(1,1h)
strtndasc
time 2m
stpndasc

gts'ELE11'
sndsacsrc(1,1h);
stabct
trkelof(60');
trksac(1,1h)
strtndasc
time 2m
stpndasc

end

```

Figure 1: A sample command file for obtaining data along a grid of points in the elevation/azimuth.

The following analysis was done on the above data to obtain eighth-order polynomial fits to the gain of the primary beamshape:

## 2.1 Step 1

The lta file is first run through *xtract* (Sanjay Bhatnagar, 1997, R00171) to extract the visibilities with the reference antenna required for subsequent analysis. The programme is invoked by saying 'xtract help=dbg' at the command line. The following typical inputs to the programme are given:

```
in           = 3c48-el-330-C12.lta
out          = beamc01el-c45.dat
scans        =
object       =
timestamps   =
baselines    = C12-USB-130
channels     = 45
antennas     =
integtime    = 1000
normalize    =
eat          = 0.2m
fmt          = ha%10.5f;base{chan{a%11.4f}};
```

Here *3c48-el-330-C12.lta* is the input lta file which contains the relevant data, *beamc01el-c45.dat* is the output ascii file that *xtract* will create, *C12* is the reference antenna and we are using the USB data of 130 MHz polarization, *45*th channel is used in the analysis, *1000* is the integration time which in this case translates to a scan average, *0.2m* is the time at the beginning of the record which is ignored and *ha%10.5f;base{chan{a%11.4f}};* specifies the format in which we desire the output. Note that the fmt should have HOUR ANGLE on the x-axis and amplitude on the y-axis and the baselines should be taken with the reference antenna ie the antenna that was kept tracking the source when the azimuth and elevation grid offsets were observed.

Now we have an output file which contains the relevant data in ascii format.

## 2.2 Step 2

The output file obtained from Step 1 is now processed through a shell script *fitpoly* which runs three tasks. It runs the C++ programme 'poly' developed for this

purpose, invokes gnuplot and thirdly runs another C++ programme 'normalize' again developed for this purpose. Since gnuplot has extensive routines for a non-linear least squares fitting of the data using the Marquardt-Levenberg algorithm, we used these by supplying only the required functional form of the eighth-order polynomial.

Before *fitpoly* is run, the parameters file POLY.PARM used by it has to be edited and appropriate inputs specified. A sample POLY.PARM shown below has the following fields:

```
beamc01el-c45.dat    #Output of xtract
beamc01elc45sq.dat  # Data in Power → arcmin format - output of poly.
elevation           #Specify whether its an ELEVATION or AZIMUTH grid
+33.1               #Declination of the source in degrees
.3305               #Observing frequency in GHz
-120.0   12.0       #Observing grid edge for first point and grid spacing; both in arcmin.
```

The statement after # is a comment in the above.

Once the parameters file is updated, the script *fitpoly* should be executed.

*fitpoly* first runs the programme *poly* which reads the ascii data file outputted by *xtract*, squares the visibility data to convert to power units and labels the x-axis in appropriate arcmin offsets. It reads the inputs from POLY.PARM. For an azimuth grid, it takes care of labelling the x-axis appropriately after taking out the cos(el) effect. The output is written in ascii format in a user-specified file (in the above example in *beamc01elc45sq.dat*). The script then invokes gnuplot and waits for user input. Since there is no automated flagging of data implemented in any of the programmes, it is a good idea at this stage to check the data in the output file in a separate window and remove any outliers. Once that is over, you need to run the gnuplot programme *run.gnu* within gnuplot. The syntax is

```
> call "run.gnu" "beamc01elc45sq.dat"
```

You need to check if run.gnu and all the files required by it are in the appropriate directory. Specify the full path for run.gnu. Similarly the second argument is the name of the file which is output by *poly*. Be careful to give both the arguments correctly. This will use the input data file and do a least squares fit to the data using the Levenberg-Marquardt algorithm. 'run.gnu' is a sequence of gnuplot commands specifying the functional form of an eighth-order polynomial and which calls in a separate window the 'fit' routine within gnuplot. The beamshapes for all the antennas in 'beamc01elc45sq.dat' are fitted by an eighth-order polynomial. 'run.gnu' also calls other gnuplot command files which it will run through without user inter-

vention. It will generate a postscript file 'beams.ps' which contains the data points and the eighth-order polynomial fits to all the primary beamshapes that gnuplot has generated. It also generates the output file 'fit.log' which contains the coefficients and the errors on those. gnuplot will run through the entire sequence of commands and wait for the next command when it is over. Type in 'exit' and the script will continue.

The third and last job in the script is to run the C++ programme *normalize* which examines the output file produced by the fitting routines within gnuplot (fit.log) and based on the standard errors generated by the routine determines whether the beamshape data and the fit are useful. The polynomial coefficients are then normalized by the constant and written out in the file 'Fit.out'. The mean values calculated from all the useful fits are also written out in this file. The scatter on the coefficient is taken as the peak-to-peak error on the coefficients.

Check the output files generated by the script:

```

beamc01elc45sq.dat  # the output from poly
fit.log              # the output file from gnuplot containing all coefficients
                    # of the polynomial fits and the standard errors on these.
tmp.out             # Output from normalize which contains the
                    # polynomial coefficients and the errors in % on these.
Fit.out             # the final output from normalize which contains the good fits,
                    # errors on these and the mean values of the
                    # coefficients which are required by PBCOR in AIPS.
beams.ps            # contains the plots of the beamshape data and the polynomial fits.

```

Please note that the primary beam gain correction can be applied to the data (with  $\lambda > .25\text{cm}$ ) using PBCOR only in the 31DEC01 and higher versions of AIPS. In the earlier versions of AIPS, a gaussian fit was used to characterize the beams for wavelengths  $> 0.25$  cm. The entire suite of programmes is available as a tar file.

### 3 Results

The suite of programmes used for fitting the 1-dimensional GMRT primary beam shapes gives the coefficients, a,b,c,d of the eighth-order polynomial:  $1 + ax^2 + bx^4 + cx^6 + dx^8$ . These coefficients are tabulated below for 610, 325 and 240 MHz. An example of the data points and the fitted polynomial to 610 MHz primary beam shapes is shown in Fig 2. The polynomial fit to the data is good in most of the

cases. The fits in panels 1 and 3 in the left hand side panels are bad and are not included in the final results.

Table 1: The coefficients for the eighth order polynomial given above are tabulated here for the three frequency bands, 610, 325 and 240 MHz. For 610 MHz, the peak-to-peak errors found from the scatter on the coefficients from fits to data from four days have been noted below the coefficient values in brackets.

<b>Freq</b> MHz	<b>Grid</b>	<b>Poln</b>	<b>a</b>	<b>b</b>	<b>c</b>	<b>d</b>
610	el	130	-0.0035311	4.81813e-06	-2.96602e-09	6.88468e-13
	el	175	-0.0035494	4.86037e-06	-2.9992e-09	6.97575e-13
	az	130	-0.0033616	4.4573e-06	-2.78041e-09	6.90297e-13
	az	175	-0.0033909	4.58005e-06	-2.97522e-09	7.91729e-13
330	el	130	-0.0028144	2.9948e-06	-1.41772e-09	2.5104e-13
240	el	130	-0.00330745	4.29698e-06	-2.5686e-09	5.87591e-13
	el	175	-0.00339308	4.67145e-06	-3.03032e-09	7.58818e-13

As can be seen in the table, we have been able to obtain good data at 610 MHz and fit both the elevation and azimuth grids for both polarizations. The coefficients match well for the 130 and 175 MHz beams. However, there does seem to be a systematic difference in coefficients ( $\leq 5\%$ ) for the elevation and azimuth beams but it is not clear at this point whether it is significant or within errors. The experiment needs to be repeated.

We did not get sufficient good data at 330 MHz and hence only the 130 MHz elevation grid data could be used to find the coefficients. The procedure certainly needs to be repeated for this frequency band.

At 240 MHz, we obtained good data for the elevation grids at both the polarizations. However, the azimuth grid data was corrupted. It would be useful to repeat the procedure for a new set of data.

In the table below, we tabulate the coefficient values that the user needs to specify in the task PBCOR inside AIPS for all the four bands.

## 4 Summary

A script has been prepared for fitting an eighth-order polynomial to the primary beam shape obtained by using cross-power for the GMRT antennas. This script *fit-poly* runs three programmes: *poly* (a C++ routine locally developed by us), *gnuplot*

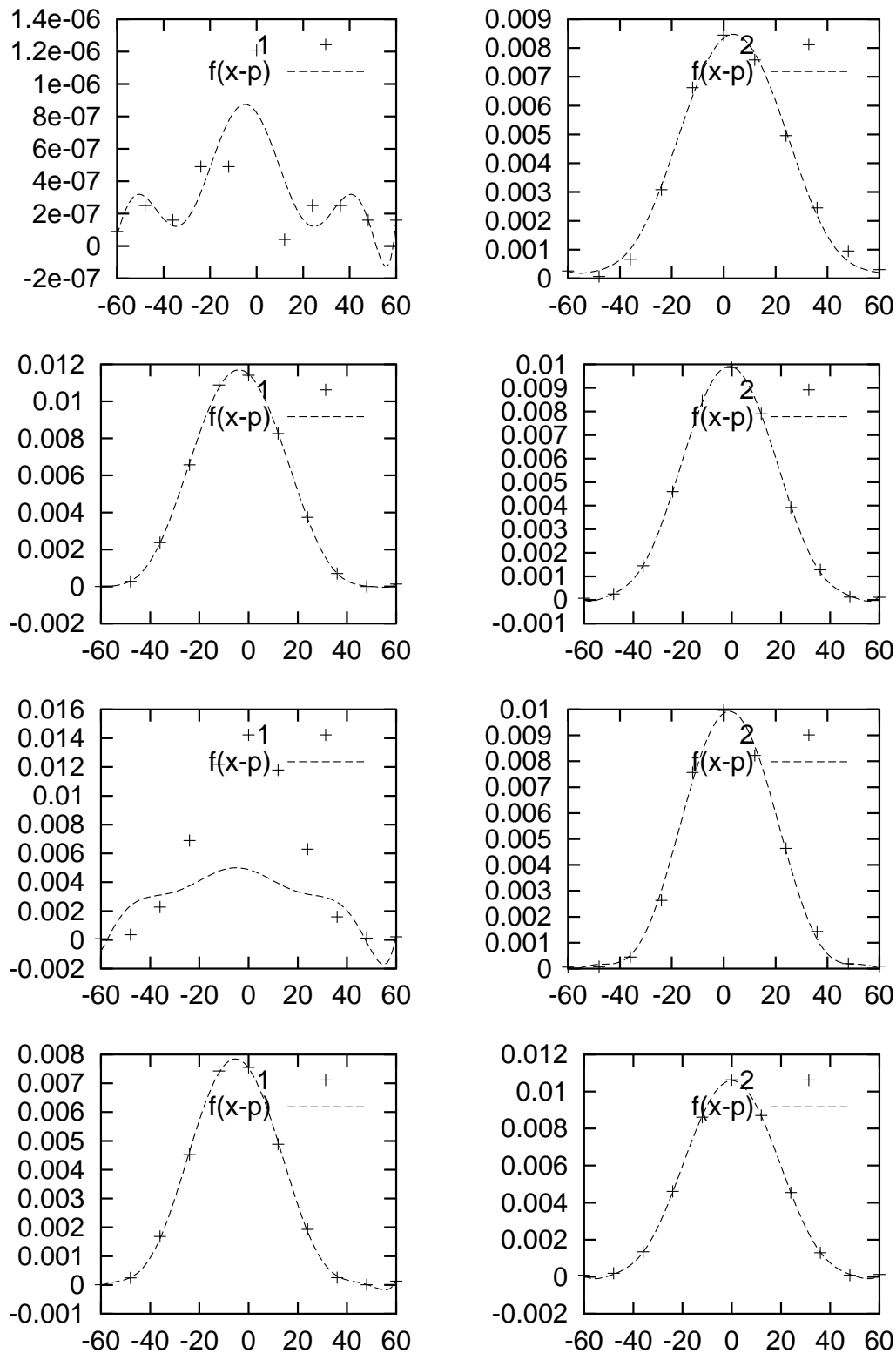


Figure 2: The figure shows the data points in crosses and the eighth-order polynomial fit to the cross-power primary beams at 610 MHz. The x-axis is labelled in arcminutes whereas the y-axis shows the cross power for that baseline. The eight panels show eight antennas, in this case C00 to C08. The first antenna fit is bad and is not used in deriving the final fit coefficients.

Table 2: The values required to be filled in the array PBPARAM in the task PBCOR in AIPS for primary beam gain correction for the four frequency bands are tabulated here.

<b>Freq</b> MHz	PBPARAM(3)	PBPARAM(4)	PBPARAM(5)	PBPARAM(6)	HPBW
1280	-2.27961	21.4611	-9.7929	1.80153	26'
610	-3.427	45.299	-26.9032	5.98777	43'
325	-2.8144	29.948	-14.1772	2.5104	87'
240	-3.36648	46.1594	-29.9625	7.52884	108'

(gnu utilities) and *normalize* (a C++ routine locally developed by us) which give the polynomial coefficients. The input data to the script is an ascii data file output by *xtract* (Sanjay Bhatnagar, 1997, R00171). In short the entire list of commands required for finding the best polynomial fit and its coefficients using a one-dimensional grid along elevation or azimuth directions consists of the following:

1. xtract
2. source fitpoly
3. gnuplot> call "run.gnu" "power-data-filename"
4. gnuplot> exit
5. Look at Fit.out for best fit and beams.ps for the fitted data plots.

This has yielded coefficient values for an eight-order polynomial fit to the observed primary beamshape at 240 MHz, 325 MHz and 610 MHz as tabulated in Table 2.